

Tissue macrophages act as cellular chaperones for vascular anastomosis downstream of VEGF-mediated endothelial tip cell induction

*Alessandro Fantin¹, *Joaquim M. Vieira,¹ Gaia Gestri,² Laura Denti,¹ Quenten Schwarz,¹ Sergey Prykhozhiy,³ Francesca Peri,³ Stephen W. Wilson,² and Christiana Ruhrberg¹

¹UCL Institute of Ophthalmology and ²UCL Department of Cell and Developmental Biology, University College London, London, United Kingdom; and ³European Molecular Biology Laboratory (EMBL), Heidelberg, Germany

Blood vessel networks expand in a 2-step process that begins with vessel sprouting and is followed by vessel anastomosis. Vessel sprouting is induced by chemotactic gradients of the vascular endothelial growth factor (VEGF), which stimulates tip cell protrusion. Yet it is not known which factors promote the fusion of neighboring tip cells to add new circuits to the existing vessel network. By combining the analysis of mouse mu-

tants defective in macrophage development or VEGF signaling with live imaging in zebrafish, we now show that macrophages promote tip cell fusion downstream of VEGF-mediated tip cell induction. Macrophages therefore play a hitherto unidentified and unexpected role as vascular fusion cells. Moreover, we show that there are striking molecular similarities between the pro-angiogenic tissue macrophages essential for vascu-

lar development and those that promote the angiogenic switch in cancer, including the expression of the cell-surface proteins TIE2 and NRP1. Our findings suggest that tissue macrophages are a target for antiangiogenic therapies, but that they could equally well be exploited to stimulate tissue vascularization in ischemic disease. (*Blood*. 2010;116(5): 829-840)

Introduction

Blood vessels are essential for tissue homeostasis in all vertebrates, and new vessel growth, termed neo-angiogenesis, is therefore a critical process in wound repair to counter tissue ischemia. Undesirably, neo-angiogenesis also promotes the expansion of tumors. Moreover, nonproductive neo-angiogenesis, which fails to restore oxygenation of ischemic tissues, promotes disease progression in, for example, diabetic retinopathy. Much current research is therefore focused on the identification of molecular and cellular targets for either pro- or antiangiogenic therapies. We previously elucidated the mechanism by which alternative splice forms of the vascular endothelial growth factor (VEGF) cooperate to promote blood vessel growth.^{1,2} This work led to the current model of angiogenesis, in which blood vessel endothelium specializes into tip and stalk cells to promote vascular network expansion by sprouting growth. While the stalk cells form a lumen to transport blood, the tip cells extend filopodia to detect chemotactic growth factor gradients, which are formed by a combination of VEGF isoforms with a differential affinity for the extracellular matrix. Cooperating with VEGF, notch-delta signaling controls the balance of tip versus stalk cell specialization.³ Even though much progress has been made in elucidating the mechanism of vascular sprout induction and guidance, a fundamental yet unanswered problem is which mechanism promotes the fusion of nascent vessel sprouts to add new circuits to the existing plexus.

Macrophages promote pathologic angiogenesis in several diseases. Thus, circulating bone marrow-derived cells differen-

tiate into proangiogenic cells with macrophage characteristics at adult sites of VEGF expression⁴ and are recruited to growing tumors to promote tumor vascularization and therefore progression.^{5,6} In several diseases, macrophages are variably detrimental or beneficial. For example, macrophages contribute to intra-aortic plaque formation in experimental models of artery occlusion, but can also promote collateral growth to alleviate ischemia.^{7,8} In the retina, tissue-resident and recruited macrophage populations have been implicated in developmental and pathologic angiogenesis.⁹⁻¹² These contradicting results raise the possibility that different subpopulations of macrophages exist whose activity could be selectively targeted for pro- or antiangiogenic therapies, provided that they are distinguishable at the molecular and functional level.

Supporting the concept of macrophage diversity, a recent study demonstrated that a subset of monocytes with a noninflammatory profile circulates in the blood of healthy adults and overlaps phenotypically with the macrophage population that promotes tumor angiogenesis.¹³ These monocytes/macrophages are characterized by expression of 2 transmembrane proteins essential for angiogenesis, the angiopoietin receptor TIE2¹⁴ and the multifunctional NRP1 protein, a receptor for specific class 3 semaphorins and VEGF isoforms that also modulates intercellular adhesion.¹⁵ An antigenically similar population of TIE2-expressing macrophages (TEMs) exists in the embryo before the production of monocyte-derived macrophages.¹³ Yet the mechanistic contribution of these TEMs to physiologic angiogenesis

Submitted December 9, 2009; accepted April 8, 2010. Prepublished online as *Blood* First Edition paper, April 19, 2010; DOI 10.1182/blood-2009-12-257832.

*A.F. and J.M.V. contributed equally to this article.

The online version of this article contains a data supplement.

The publication costs of this article were defrayed in part by page charge payment. Therefore, and solely to indicate this fact, this article is hereby marked "advertisement" in accordance with 18 USC section 1734.

© 2010 by The American Society of Hematology

has not been explored. We demonstrate here that yolk sac-derived macrophages expressing TIE2 and NRP1 comprise the major population of tissue macrophages at the time of brain vascularization, and that they interact with endothelial tip cells to promote vascular anastomosis downstream of VEGF-mediated tip cell formation and sprout induction. Our findings therefore provide fundamental mechanistic insight into the control of vessel fusion during angiogenesis and draw surprising parallels between developmental tissue vascularization and the angiogenic switch in cancer.

Methods

Animals

We used mice with a knockout mutation for *Pu.1* (*Sfp1*),¹⁶ an inactivating point mutation in *Csfl* (*Csfl^{Op/Op}*),^{17,18} a knock-in mutation abrogating the heparin-binding VEGF isoforms (*Vegfa^{120/120}*);¹ a floxed *Vegfa* conditional null allele (*Vegfa^{fl/+}*) or a *Lysm^{Cre}* or *Nes^{Cre}* transgene.¹⁹⁻²¹ We also used mice carrying a floxed yellow fluorescent protein (YFP) reporter or diphtheria toxin gene in the *Rosa26* locus.^{22,23} Mice were mated in the evening, and the morning of vaginal plug formation was counted as 0.5 days postcoitum (dpc). Embryos from different litters were stage-matched by comparing facial and limb development. All animal research was conducted with United Kingdom Home Office and ethical approval.

To visualize macrophages in living zebrafish embryos, we modified a published construct that expresses green fluorescent protein (GFP) under the control of the *Pu.1* promoter²⁴ to express red fluorescent protein (RFP; *Pu.1:Gal4-UAS-TagRFP*). Two nanoliters of this construct together with *Tol2* RNA were injected at a final concentration of 25 ng/ μ L each into fertilized *Tg(fli1a:EGFP)^{y5}* eggs,²⁵ and eggs were then incubated at 28°C. For live imaging, embryos were treated with phenylthiourea at 24 hours postfertilization (hpf) to prevent melanization, and at 28 hpf anesthetized in 0.01% tricaine and embedded in 1.5% low-melting-point agarose. Time-lapse analysis was carried out on a Leica SPE confocal microscope with a 40 \times objective with a numerical aperture (NA) of 0.8 by acquiring z-stacks through the relevant body region every 3 minutes. The z-stacks were flattened by maximum projection and arranged in a time series using Volocity software (Improvision).

Immunolabeling and quantification of vessel and macrophage density

The following antibodies were used: rat anti-platelet endothelial cell adhesion molecule (PECAM) and anti-CD11b (BD PharMingen), rat anti-F4/80 (Serotec), rabbit anti-IBA1 (WAKO), anti-GFP (MBL), anti-collagen IV (Serotec) or anti-activated caspase 3 (Millipore), goat anti-rat NRP1 (R&D Systems) or anti-mouse TIE2 (R&D Systems) and mouse anti- α smooth muscle actin (Sigma-Aldrich), Alexa-conjugated goat anti-rat or anti-rabbit IgG (Molecular Probes) and Cy3-conjugated rabbit anti-goat Fab fragment (Jackson Immuno). In some experiments, anti-PECAM was detected by horseradish peroxidase (HRP)-conjugated rabbit anti-rat IgG (DAKO), and biotinylated isolectin B4 (IB4; Sigma-Aldrich) by Alexa-conjugated streptavidin (Molecular Probes) or streptavidin-HRP (DAKO). Samples were imaged with a Zeiss LSM510 laser scanning confocal microscope or a Leica MZ16 stereomicroscope equipped with a ProgRes C14 digital camera (Jenoptiks). The following objectives were used on the LSM510 microscope: 10 \times , NA 0.3; 20 \times , NA 0.5; 40 \times , NA 1.3; 63 \times , NA 1.4. Images were processed with Adobe Photoshop CS3 (Adobe Inc). Three-dimensional surface rendering of high-resolution confocal z-stacks was carried out with Volocity (Improvision). The number of intersections, tip cells, radial vessels and macrophages in hindbrains, or intersections and regression profiles in

the retina were determined in 3 randomly chosen regions (0.2 mm² for confocal, 0.25 mm² for bright-field images of hindbrains, and 0.05 mm² for retinal samples). For each genotype or time point, we determined the mean of 3 to 10 independent samples; error bars represent the standard deviation of the mean. To determine whether 2 datasets were significantly different, we calculated the *P* value by performing a 2-tailed unpaired *t* test; in experiments comparing 3 datasets, we additionally performed a 1-way ANOVA followed by a Tukey post-hoc test. Statistical significance is reported in the figures (**P* < .05; ***P* < .01; ****P* < .001).

RT-PCR

Total RNA was extracted with Tri-Reagent (Sigma-Aldrich), and contaminating DNA was removed with RNase-free DNase (Promega). First-strand cDNA was synthesized with Superscript Reverse Transcriptase II (Invitrogen). RT-PCR was performed with the following oligonucleotide primers: *Pu.1* 5'-TACCAACGTCCAATGCATGA-3' and 5'-CTCCAAGCCATCAGCTTCTC-3'; *Csfl* 5'-ATGGACACCTGAAGGTCCTG-3' and 5'-ATGGAAAAGTTCGGACACAGG-3'; *Actb* 5'-CTCTTCCAGCCTTCTCTCCTG-3' and 5'-GAAGCATTTCGGGTGGACGAT-3'; pan-*Vegfa*: 5'-ATGAACTTCTGCTCTCTTGG-3' and 5'-TCACCGCCTTGGCTTGTCACA-3'. Quantitative real-time PCR was conducted with the Power SYBR Green PCR Master Mix on a 7900HT Fast Real-Time PCR System (Applied Biosystems) with the following primers: pan-*Vegfa* 5'-GACTTGTGTTGGGAGGAGGA-3' and 5'-TCTGGAAGTGAGCCAATGTG-3'; *Actb* 5'-TCCAAGTATCCATGAAATAAGTGG-3' and 5'-GCAGTACATAATTTACACAGAAGC-3'. Negative controls contained RNA template not subjected to reverse transcription. Data were collected using Sequence Detector software (SDS version 2.2; Applied Biosystems) and analyzed using DART-PCR software.²⁶ *Vegfa* expression was normalized using *Actb* as a reference.

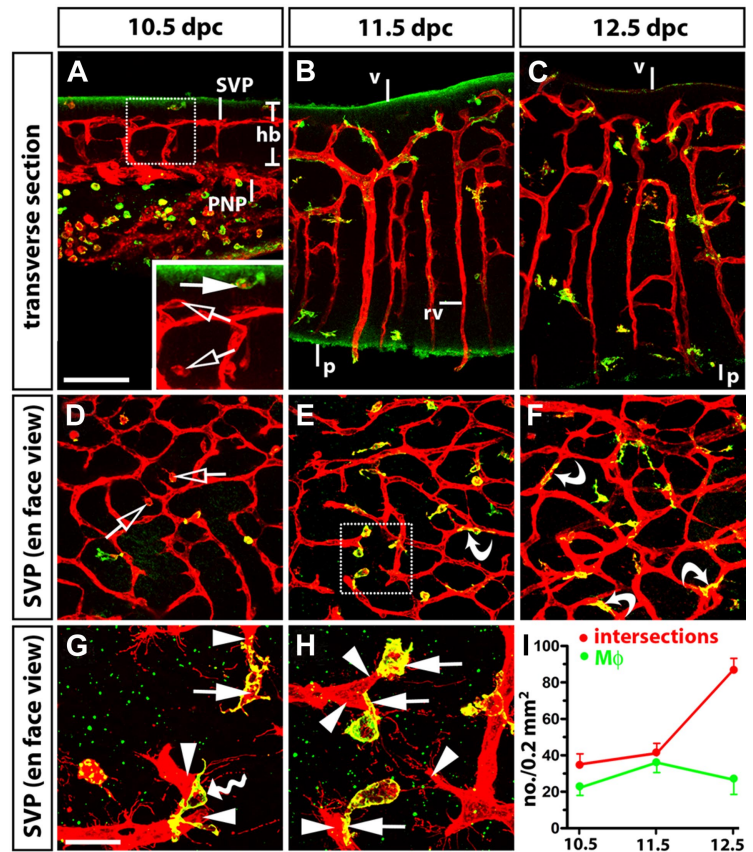
Results

Spatiotemporal association between macrophages and sprouting vessels

In the adult, macrophages originate from bone marrow-resident hematopoietic stem cells via circulating intermediates known as monocytes. In contrast, the first embryonic macrophages appear in the yolk sac well before any other leukocytes, and they differentiate in a rapid pathway that bypasses the monocytic stage.²⁷⁻²⁹ These early macrophages travel from the yolk sac into the embryo proper before the circulation is established, and they therefore predate the first monocyte-derived macrophages, which originate in the aortogonad-mesonephros region and liver and enter the brain by extravasation. We reasoned that the embryonic hindbrain was ideally suited to study the role of the early, yolk sac-derived macrophages in angiogenesis, because avian studies had demonstrated that they colonise the brain by crossing the pial membranes and roof plate concomitantly with, but independently of, blood vessels.^{30,31}

Using the dual blood vessel/macrophage marker IB4 in combination with the macrophage-specific markers F4/80 and IBA1,^{29,32,33} we confirmed that yolk sac-derived macrophages colonized the embryonic mouse brain independently of vessels, as reported for the chick (supplemental Figure 1, available on the *Blood* Web site; see the Supplemental Materials link at the top of the online article). We found that embryonic brain macrophages were always IB4-positive and that they expressed F4/80 by 11.5 dpc (Figure 1A-E; supplemental Figure 1). We further observed that they rapidly established a close association with sprouting vessels in the brain parenchyma. Thus, macrophages accumulated in the subventricular

Figure 1. Spatiotemporal relationship of tissue macrophages and blood vessels during angiogenesis in the developing hindbrain. Eighty-micron transverse sections (A-C) and whole mounts (D-H) of 10.5-, 11.5-, and 12.5-dpc wild-type hindbrains, labeled for IB4 (red) and F4/80 (green). Solid white arrows indicate macrophages positive for both markers; clear arrows, macrophages positive for IB4 only; curved arrows, macrophages embracing vascular intersections; arrowheads indicate endothelial tip cells. (G-H) Higher magnifications of the SVP illustrate the interaction of tip cells (arrowheads) with macrophages (arrows) and the bridging of neighboring tip cells by a macrophage (wavy arrow in G; note that one of the 2 vessel sprouts emerges from a deeper plane of section); panel H shows a higher magnification of the boxed area in panel E. Scale bars: panels A through F, 100 μ m; panels G and H, 25 μ m. V indicates ventricular brain surface; p, pial brain surface; rv, radial vessels; hb, hindbrain; SVP, subventricular vascular plexus; and PNP, perineural vascular plexus. (I) Quantitation of macrophages (M ϕ , green) and vascular intersections in the SVP (red) between 10.5 and 12.5 dpc; n \geq 15. Error bars represent SD of the mean.



zone (SZ) between 10.0 and 11.5 dpc, when vessels began to sprout laterally and fused with neighboring vessel branches to form the subventricular vascular plexus (SVP; Figure 1A-B and supplemental Figure 1B). Moreover, the number of macrophages in the SZ peaked at 11.5 dpc, the major phase of vascular networking (Figure 1B,E,I). Correlating with the time point when the SVP had become established, the macrophage number in the SZ declined (compare samples at 11.5 and 12.5 dpc; Figure 1C,F,I). Concomitantly with their decrease in the SZ, macrophages began to accumulate in the deeper brain layers, and this shift in distribution correlated with the formation of connections between neighboring radial vessels from 11.5 dpc onwards (compare Figure 1B with Figure 1C).

During all phases of vascular networking, macrophages appeared to interact with endothelial tip cells (Figure 1G-H). In some instances, macrophages bridged neighboring tip cells, as if to align them in preparation for fusion (Figures 1G and 2A). As the SVP became more complex, macrophages often localized to vessel junctions, where they embraced joining vessel segments (curved arrows in Figures 1E-F and 2B). Three-dimensional surface rendering of high-resolution confocal z-stacks of hindbrains in the main phase of vascular networking illustrated the interaction of macrophages with filopodia on opposing tip cells more clearly (Figure 2C,C'), and further revealed that macrophages remained in contact with vessel junctions for at least some time after vessel sprouts had fused to form a vascular intersection (Figure 2D,D'). Together, these observations suggest that macrophages adopt strategic positions consistent with a role in promoting vessel fusion.

Essential role for tissue macrophages in embryonic angiogenesis

To establish if macrophages play an essential role in vascular networking, we studied mice carrying a loss-of-function mutation in the gene encoding the transcription factor PU.1,¹⁶ which regulates the expression of myeloid proteins such as the integrin CD11b (MAC-1, CD18) and the receptor for the macrophage colony-stimulating factor CSF1 (M-CSF).³⁴ Loss of PU.1 therefore severely compromises the development of monocyte-derived macrophages, but mice do not suffer obvious brain abnormalities.^{16,35} Because it was reported that these mice retain some primitive “macrophage-like” cells that express the CSF1 receptor,^{36,37} we first examined if early tissue macrophages were present in these mice. We found that mouse embryos lacking PU.1 did not contain any F4/80- or IBA1-positive tissue macrophages in the head mesenchyme or hindbrain parenchyma at 11.5 dpc (supplemental Figure 2). This observation confirmed that PU.1 is a master regulator for the differentiation of both monocyte- and yolk sac-derived macrophages.

The analysis of *Pu.1*-null hindbrains revealed that macrophage deficiency significantly reduced the number of vessel intersections and thereby decreased SVP complexity (compare Figure 3A with B; Figure 3D). Fewer connections also formed between neighboring radial vessels in mutant compared with wild-type hindbrains at the time when vascular networking was initiated in deeper brain layers (compare Figure 3I with J; Figure 3L). These findings suggest that early tissue macrophages play an essential role in brain angiogenesis. However, the SVP defect of PU.1 knockouts was less severe than that of *Vegfa*^{120/120}

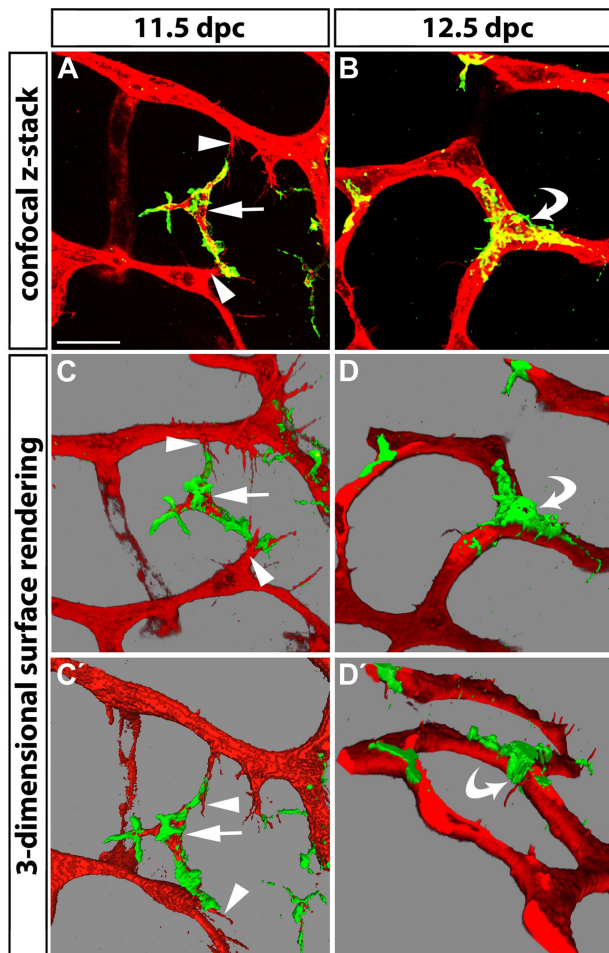


Figure 2. Tissue macrophages bridge endothelial tip cells and are present at vascular junctions. Hindbrains from 11.5- and 12.5-dpc wild-type embryos were fluorescently labeled with IB4 (red) and F4/80 (green) to reveal the relationship of endothelial cells (red) and macrophages (double-positive, yellow) in the subventricular zone. (A) A macrophage (arrow) interacts with the filopodia of 2 opposing tip cells (arrowheads) at E11.5. (B) A macrophage embraces a 3-way junction, the product of vessel fusion (curved arrow). (C-D) Snapshots of 3-dimensional models obtained by surface rendering of the confocal z-stacks shown in panels A and B. Panels C' and D' show different angles of the models shown in panels C and D, respectively. Scale bar represents 25 μ m.

mutants, which lack the heparin-binding VEGF isoforms VEGF164 and VEGF188 and are therefore defective in forming chemoattractive VEGF gradients for vessel sprouting and guidance¹ (compare Figure 3B with C; Figure 3D).

The detailed comparison of the different stages of hindbrain vascularization suggested that the vascular defects in both types of mutants arose by a different mechanism. First, vessel sprouting from the perineural plexus into the brain was strongly reduced in *Vegfa*^{120/120}, but not in *Pu.1*-null mutants (compare Figure 3E with F-G; Figure 3H). Second, radial vessels had hardly sprouted laterally in the deeper layers of *Vegfa*^{120/120} hindbrains at 12.5 dpc (Figure 3K), but such sprouts were present in macrophage-deficient brains (Figure 3J). Third, *Vegfa*^{120/120} hindbrains contained significantly fewer tip cells (Figure 3O), as previously reported,¹ but the number and morphology of tip cells appeared normal in *Pu.1*-null hindbrains (Figure 3N,P). Thus, the reduced vascular complexity of *Vegfa*^{120/120} hindbrains is due to a cumulative reduction of vessel sprouting, which occurs initially at the level of sprout invasion

into the brain (Figure 3G), then at the level of sprouting within the SZ (Figure 3C,O) and finally at the level of sprouting in the deeper layers (Figure 3K). Even though there were significantly fewer tip cells in *Vegfa*^{120/120} hindbrains, macrophages still interacted with the few tip cells that were present (Figure 3O; see also Figure 5D). In contrast, *Pu.1*-null mutants did not appear defective in tip cell induction or sprouting, but specifically in vascular anastomosis. Therefore, it seems likely that vascular anastomosis is reduced in *Vegfa*^{120/120} mutants because fewer tip cells are available for fusion, while vascular anastomosis in *Pu.1*-null mutants is reduced, because macrophages do not align tip cells in preparation for fusion.

The recruitment of proangiogenic brain macrophages requires CSF1

Because PU.1-deficient mice are defective in B-cell development in addition to macrophage differentiation, we complemented our study by analyzing mice that carry an inactivating mutation in the *Csf1* gene (*Csf1*^{Op/Op}).¹⁷ This mutation impairs the production of monocyte-derived macrophages, but, unlike the *Pu.1*-null mutation, does not impair B-cell development or T cell-mediated immunity.³⁸ We found that CSF1 deficiency decreased, but did not abolish the formation of embryonic tissue macrophages (supplemental Figure 3A-B). However, CSF1 deficiency severely disrupted the recruitment of macrophages from the head mesenchyme into the brain (supplemental Figure 3A-D). Because *Csf1* was expressed in the hindbrain at the time of macrophage recruitment (supplemental Figure 3F) and CSF1 is a known chemoattractant for macrophages in vitro,³⁹ CSF1 likely mediates the recruitment of proangiogenic macrophages into the developing brain. Consistent with this idea, CSF1-deficient hindbrains had an SVP with reduced complexity, similar to *Pu.1*-null mice (supplemental Figure 3B-E).

Monocyte-derived macrophages are not essential for embryonic angiogenesis

Loss of PU.1 or CSF1 also perturbs the production of monocyte-derived macrophages, which differentiate after the onset of liver hematopoiesis at 10.5 dpc and may enter the brain by extravasation, once perfused vessel circuits have been established. To address whether monocyte-derived macrophages also contributed to vascular networking, we took advantage of a tool that selectively targets these cells, a knock-in mouse containing a *Cre* transgene in the endogenous *Lysm* locus (*Lysm*^{Cre})²⁰ that is expressed only after the onset of liver hematopoiesis.³⁶ A YFP reporter that monitors CRE-mediated recombination (*Rosa26*^{YFP})²² demonstrated that *Lysm*^{Cre} effectively targeted circulating monocytes in the embryonic brain (supplemental Figure 4B). In contrast, this promoter was active in very few tissue macrophages during the time of SVP formation (supplemental Figure 4C-D). When we eliminated monocyte-derived macrophages by activating *Lysm*^{Cre}-mediated diphtheria toxin expression from the floxed *Rosa26* locus (*Rosa26*^{DTA}),²³ tissue macrophages were spared, and the SVP reached normal complexity (supplemental Figure 4E-G). This finding demonstrated that yolk sac-derived tissue macrophages, not macrophages derived from circulating monocytes, promote brain angiogenesis.

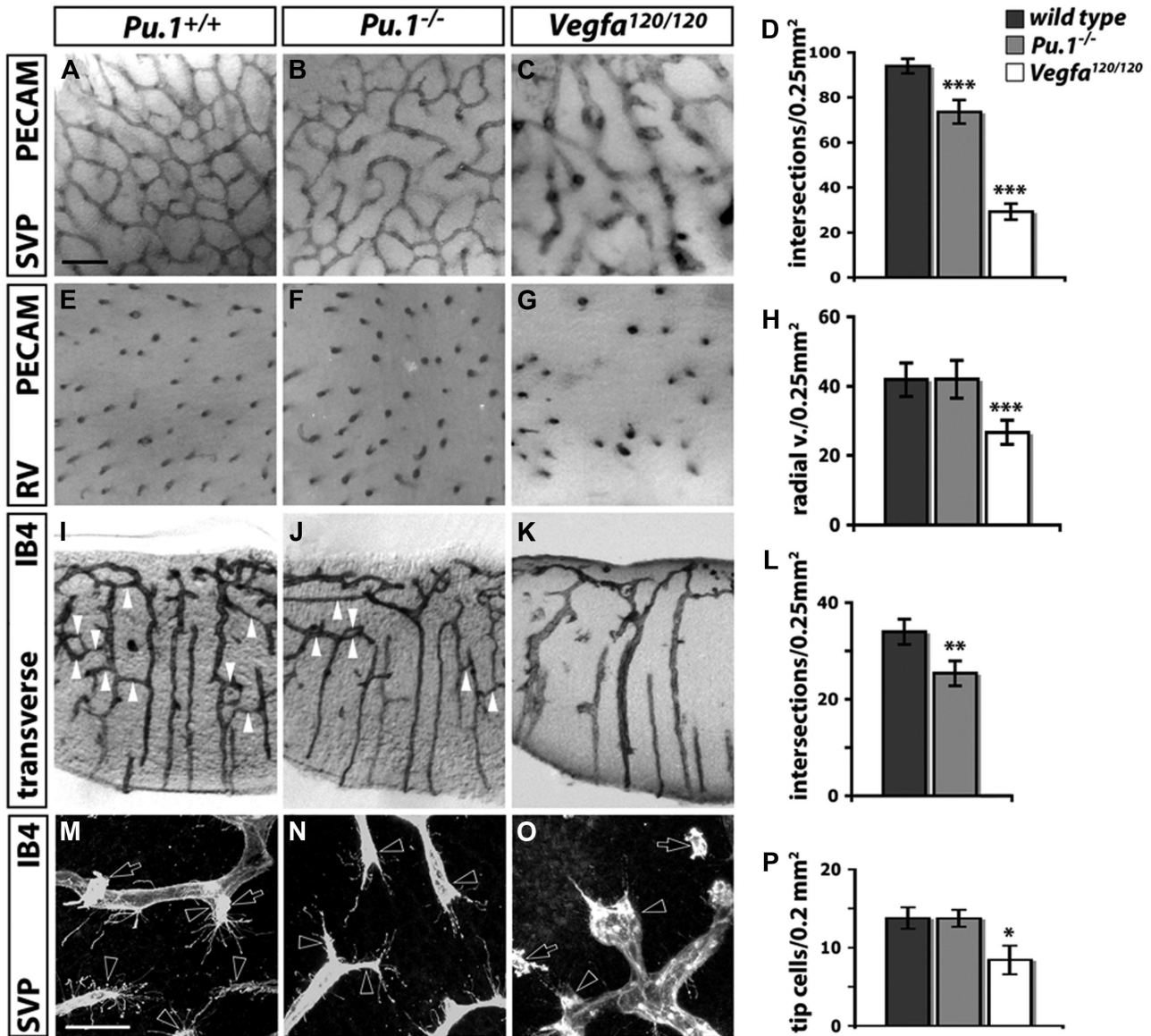


Figure 3. Brain angiogenesis is impaired in the absence of macrophages. Angiogenesis in hindbrains lacking PU.1 (*Pu.1*^{-/-}) or heparin-binding VEGF isoforms (*Vegfa*^{120/120}) at 12.5 dpc (A-L) and 11.5 dpc (M-P). (A-G) Whole mount view onto the SVP (A-C) or radial vessels (RV) diving into the brain parenchyma (E-G), visualized by PECAM immunohistochemistry (IHC) in a 0.25-mm² area. (I-K) Transverse sections (100 μm) of IB4-labeled hindbrains show vascular bridges (white arrowheads) between neighboring radial vessels. (M-O) IB4-positive endothelial tip cells (clear arrowheads) and macrophages (clear arrows) in the whole-mounted SVP. Scale bars represent 100 μm (A-K) and 50 μm (M-O). (D,H,L,P) Quantitation of the number of vascular intersections in the SVP (D; n = 5), the number of radial vessels (H; n = 5), and the number of vascular bridges between radial vessels (L; n = 3). Error bars represent SD of the mean. *P* values were determined by comparing the measurements obtained for both types of mutants to the control, which contained the measurements obtained for wild-types from both groups.

Macrophages promote brain angiogenesis independently of VEGF

Because VEGF functions as a macrophage chemoattractant in vitro,⁴⁰ we next asked if it contributed to the recruitment of angiogenic macrophages, as observed for CSF1 (supplemental Figure 3). In the developing brain, a combination of both heparin- and non-heparin-binding VEGF isoforms is normally expressed by neural progenitors in the SZ, and reducing the expression of all VEGF isoforms in these cells by targeting one *Vegfa* allele curbs vessel sprouting into the brain.^{41,42} Because the targeting of both *Vegfa* alleles with *Nes*^{Cre}-mediated CRE/LOX recombination causes lethality before brain vascularization due to transgene activity early in embryogenesis,⁴¹ we disrupted only one *Vegfa* allele with *Nes*^{Cre} to examine if reducing VEGF levels in the SZ inhibited the

corecruitment of pro-angiogenic macrophages and vessel sprouts. For this experiment, we used a *Nes*^{Cre} transgene that is active earlier in brain development than the one previously used²¹ and effectively disrupts the expression of VEGF (supplemental Figure 5).¹ Consistent with previous observations,⁴¹ the reduction of VEGF expression by neural progenitors significantly impaired vessel sprouting (Figure 4). Thus, blood vessels in the SZ of *Nes*^{Cre} *Vegfa*^{+/-} hindbrains were thin, branched infrequently, and had tip cells that extended few filopodia (Figure 4B,E,G). In contrast, reducing VEGF expression did not impair the recruitment of tissue macrophages into the SZ (Figure 4B,E,G).

In a complementary approach, we evaluated macrophage recruitment into *Vegfa*^{120/120} hindbrains, which specifically lack the main chemotactic VEGF isoform for macrophages,

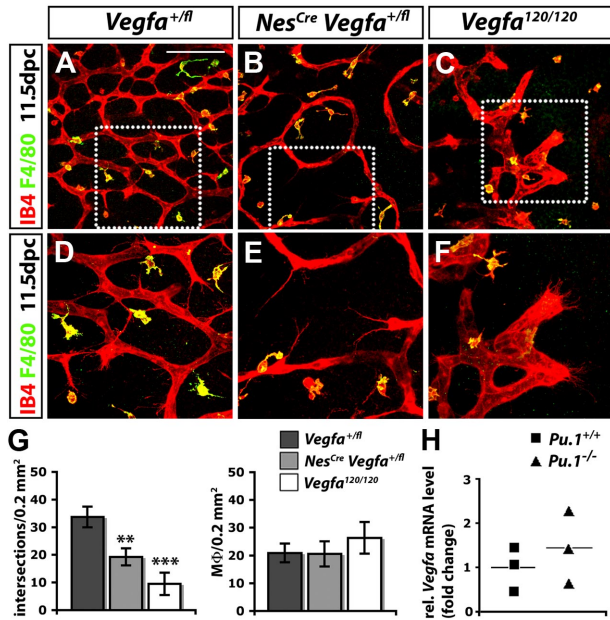


Figure 4. Macrophages promote SVP angiogenesis independently of VEGF. (A-F) Hindbrains (11.5 dpc) were labeled for IB4 and F4/80; (D-F) higher magnifications of the boxed areas in (A-C). Controls (no *Cre*; A, D) were compared with littermates with a knockdown of VEGF in neural progenitors (*NesCre Vegfa*^{fl/+}; B, E) and stage-matched mutants lacking VEGF164 only (*Vegfa*^{120/120}; C, F). Scale bar represents 100 μ m. (G) Quantitation of the number of vascular intersections and macrophages (M Φ) in the SZ at 11.5 dpc; n = 3. Error bars represent SD of the mean. The *P* values were determined by comparing both types of mutants to *Vegfa*^{fl/+} hindbrains lacking *Cre*. (H) Quantitation of *Vegfa* mRNA levels relative to *Actb* (β -actin) in *Pu.1*-deficient and wild-type littermate hindbrains at 11.5 dpc. The horizontal lines indicate the mean; n = 3.

VEGF164.⁴⁰ This mutation disrupted vascularization of the SZ even more severely than the heterozygous loss of VEGF from neural progenitors (compare Figure 4B with C; Figure 4G), but it did not impair macrophage recruitment (Figure 4C, G). Rather, there was a small, but not statistically significant increase in the number of macrophages in the lateral edge of the posterior hindbrain, an area that is hypoxic in mutants due to severe vascular deficiency (Figure 4G and data not shown). Taken together, our genetic analyses suggest that CSF1, rather than VEGF164, appears to be the main chemoattractant that recruits macrophages into the developing brain.

We next asked whether macrophages provide an important source of VEGF that complements the neural progenitor–derived VEGF pool. However, *Vegfa* levels were not reduced in *Pu.1*-null hindbrains (Figure 4H). Moreover, a reporter mouse that monitors sites of *Vegfa* expression⁴³ did not highlight any macrophages in the SZ between 10.5 and 13.5 dpc (A.F., Q.S., and C.R., unpublished observations, October 2009).¹ It therefore appears unlikely that macrophages contribute to brain angiogenesis by providing an important source of VEGF. In summary, our evidence points *against* a role for VEGF in macrophage-mediated vessel fusion during developmental angiogenesis.

VEGF-mediated tip cell guidance and macrophage-mediated sprout fusion are discrete but complementary steps that ensure proper brain vascularization

Because VEGF was not required for macrophage recruitment into the angiogenic brain, and embryonic brain macrophages did not make an obvious contribution to the angiogenic VEGF pool,

we hypothesized that VEGF-mediated sprout induction and macrophage-mediated sprout fusion are separate but complementary steps during brain angiogenesis. To test this idea, we generated mutants defective in both processes by mating heterozygous *Vegfa*¹²⁰ and *Csf1*^{Op} mice to each other and then interbreeding the double-heterozygous offspring. As predicted, the compound null mutant offspring of these mice suffered more severe defects in brain angiogenesis than littermates carrying solely one type of homozygous mutation (Figure 5). Thus, *Vegfa*^{120/120} *Csf1*^{Op/Op} double-null mutants contained many enlarged and blind-ended vessels in the SZ due to the *Vegfa*^{120/120} mutation (arrowheads in Figure 5D-E), but, in addition, anastomosis between neighboring vessel units was reduced more strongly than in single *Vegfa*^{120/120} or *Csf1*^{Op/Op} mutants (compare Figure 5B, D with E).

The great severity of vascular defects in compound mutants compared with single mutants suggested that an abundance of both tip cells and macrophages is essential for optimal vascular anastomosis. In further support of this idea, and correlating with the complete absence of brain macrophages in the *Pu.1*^{-/-} mutants, the defects of *Vegfa*^{120/120} mice carrying the *Pu.1*-null mutation appeared even more severe than those of *Vegfa*^{120/120} mice with the *Csf1*^{Op/Op} mutation (compare Figure 5E with Figure 5F). Thus, the combined disruption of VEGF gradients and macrophage-mediated vessel fusion reduced the number of vascular intersections in the SVP significantly more than the disruption of either process alone (Figure 5G). The finding that the simultaneous loss of heparin-binding VEGF and macrophages is additive leads us to propose a model, in which VEGF gradients promote tip cell formation, and

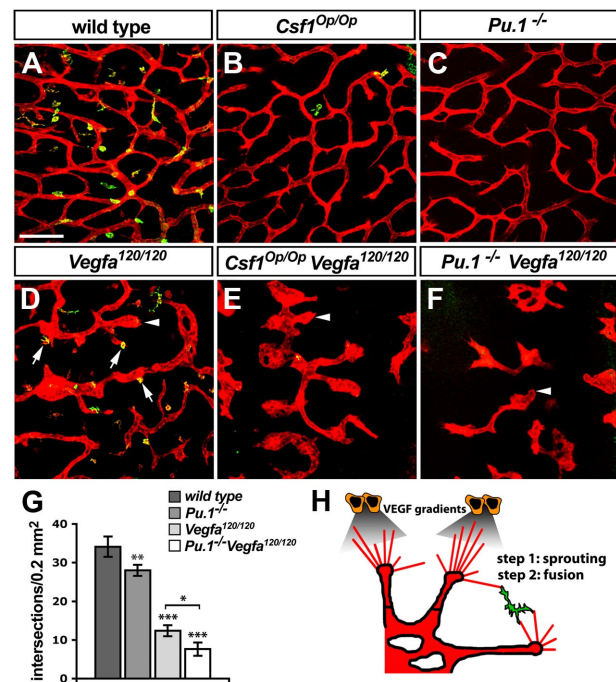


Figure 5. VEGF-induced vessel sprouting and macrophage-mediated anastomosis act synergistically to promote vascular network formation. (A-F) Morphology of the SVP (IB4-positive, red) and distribution of tissue macrophages (IB4/F4/80-double positive, yellow) in 11.5 dpc hindbrains of the indicated genotypes; arrows in panel D indicate macrophages interacting with endothelial tip cells in *Vegfa*^{120/120} mutants; arrowheads in panels D through F denote examples of bulbous vessel ends, typical of *Vegfa*^{120/120} mutants. Scale bar represents 100 μ m. (G) Quantitation of the number of vascular intersections in the SZ of the indicated genotypes at 11.5 dpc; n > 3. Error bars represent SD of the mean. (H) Schematic illustration of the role of macrophages during hindbrain vascularization.

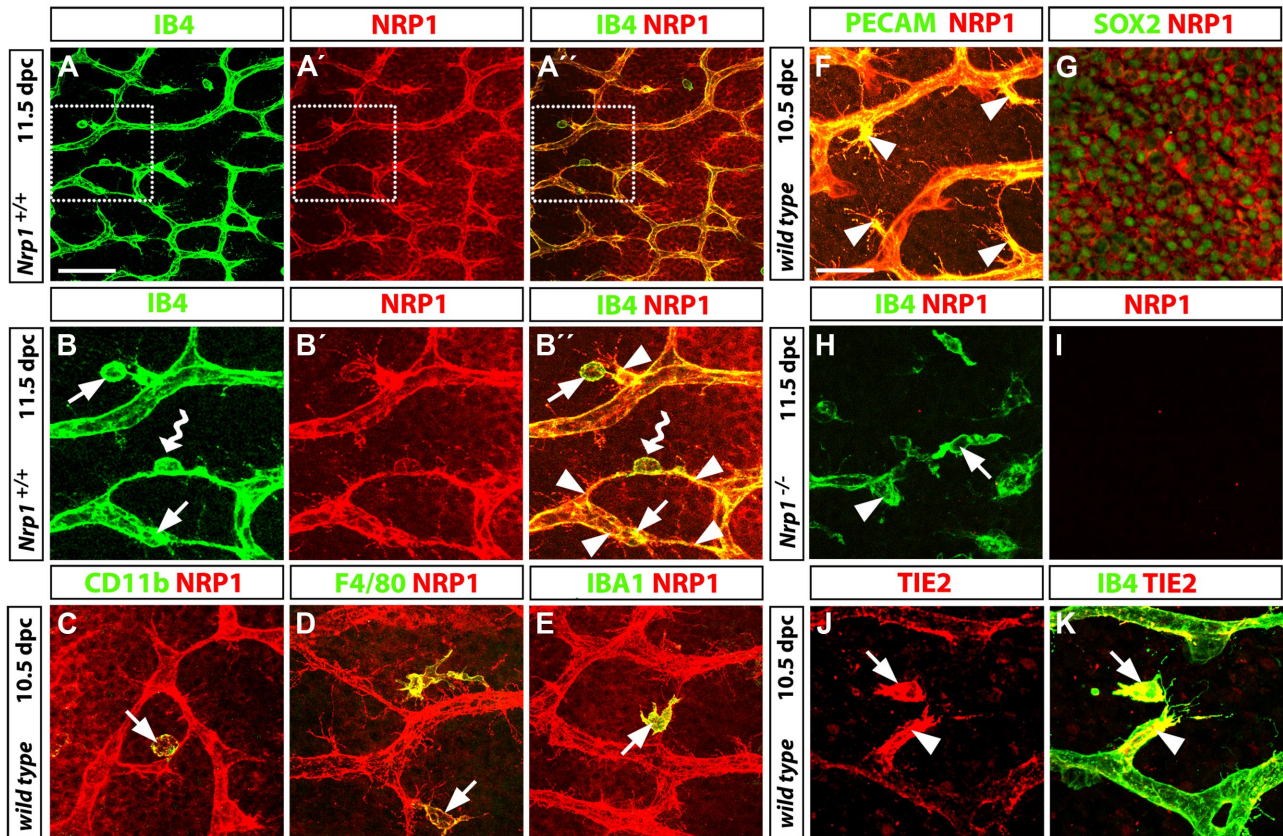


Figure 6. TEM antigen expression by proangiogenic hindbrain macrophages. (A-B) Wild-type hindbrains (11.5 dpc) were double-labeled for IB4 and NRP1 to visualize the subventricular zone, including the SVP; the boxed areas in panels A, A', and A'' are shown in higher magnifications in panels B, B', and B'', respectively; yellow indicates colocalization in panels A'' and B''. Many NRP1-positive macrophages (arrows in B, B') interacted with endothelial tip cells (arrowheads in panel B''); a NRP1-positive macrophage bridging neighboring tip cells is indicated with a wavy arrow in panels B and B'. (C-G) Double labeling for NRP1 and the macrophage markers CD11b (CD18/MAC-1), F4/80, or IBA1 (C-E), the vascular endothelial marker PECAM (F), or the neural progenitor marker SOX2 (G) established that NRP1 was expressed in all 3 cell types. Yellow indicates coexpression of NRP1 with macrophage and endothelial markers on the cell surface; in contrast, NRP1 surrounds the SOX2-positive neural progenitor nuclei. The images shown in panels F and G are stacks through the SVP or neural progenitor layer only. (H-I) The specificity of the NRP1 antibody was established by immunolabeling a *Nrp1*-deficient hindbrain, obtained from a littermate embryo of the wild-type shown in panels A and B. (J-K) Like NRP1, TIE2 (red) colocalized with IB4 (green) on a filopodia-bearing endothelial tip cell (arrowhead) and interacting tissue macrophage (arrow). Scale bars represent 25 μ m (except A-A'', 100 μ m).

macrophages act subsequently on these VEGF-induced tip cells to promote their anastomosis (Figure 5H).

The macrophages that promote vascular network formation are antigenically more similar to TEMs than inflammatory macrophages

TIE2 and NRP1 are 2 genes recently found to be significantly up-regulated in proangiogenic, but not inflammatory tumor macrophages.¹³ To address if the tissue macrophages we identified as promoters of developmental angiogenesis are functionally related to the TIE2-expressing macrophages known as TEMs, we immunolabeled embryonic hindbrain tissue with antibodies specific for NRP1 and TIE2 (Figure 6). As expected, but not shown before, we found that NRP1 was expressed in both endothelial stalk cells and tip cells, where it was particularly prominent on tip cell filopodia (Figure 6A-F). In addition, NRP1 was expressed on the surface of the majority of tissue macrophages (arrows in Figure 6A-E) and neural progenitors (Figure 6G). The specificity of the antibody used was established by staining of *Nrp1*-null hindbrain tissue; thus, the endothelial cells in the few abnormal vessels typical of these mutants were labeled by IB4, but not by the NRP1 antibody, and the same was true for tissue macrophages (Figure 6H-I). Similar to

NRP1, TIE2 was coexpressed in endothelial cells and tissue macrophages during sprouting angiogenesis in the brain (Figure 6J-K). Even though TIE2 expression was heterogeneous within the vasculature, TIE2 levels appeared to be particularly high in some nascent sprouts and their interacting macrophages. In contrast, the proangiogenic embryonic tissue macrophages do not appear to express FLT1/VEGFR1 (data not shown), even though this VEGF receptor is a marker for bone marrow-derived macrophages that promote pathologic angiogenesis.⁴⁴

Macrophages in vascular patterning during perinatal angiogenesis

To provide evidence that macrophages play a role in vascular network formation beyond early embryogenesis, we studied a second widely used angiogenesis model, the postnatal mouse retina. Like the brain, the eye is invaded by yolk sac-derived macrophages during embryogenesis (Figure 7A). Macrophage colonization of the retina therefore takes place long before its vascularization, which begins at birth, when vessel sprouts emerge from the optic nerve head and spread perpendicularly over the surface of the retina; further sprouting is then directed downwards into the inner layers of the retina, where sprouts fuse

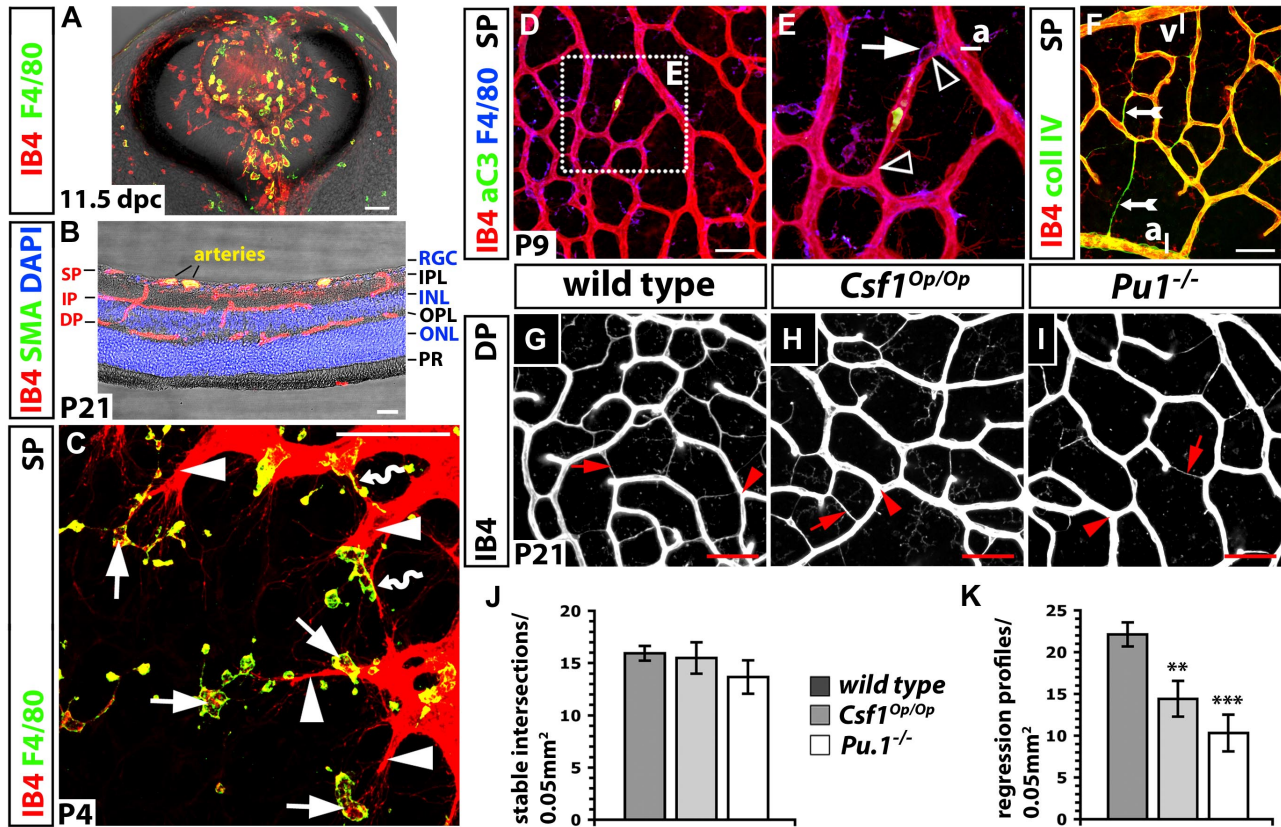


Figure 7. Retinal angiogenesis is impaired in the absence of tissue macrophages. Double-labeling of transverse sections through a wild-type mouse eye at 11.5 dpc (A) and a wild-type mouse retina at P21 (B) with IB4 and F4/80 (A) or an antibody specific for smooth muscle actin (SMA); cell nuclei in panel B were labeled with DAPI. (C-I) Whole mount labeling of the wild-type retinal vasculature at P4 (C), P9 (D-F) and P21 (G-I). (C) Some macrophages (solid arrows) interact with endothelial tip cells (solid arrowheads) at the vascular front; others embrace emerging vascular bridges (wavy arrows). (D-E) Activated caspase 3 (aC3) is present in regressing vessel segments near arteries (yellow); note capillary narrowing at the junction of the regressing vessel segment with a stable vessel (open arrowheads) and a macrophage at one of the narrow ends (solid arrow); the area boxed in panel D is shown at higher magnification in panel E. (F) Collagen IV and IB4 expression are retained by acellular capillaries (feathered arrow). (G-I) IB4-positive vessel regression profiles (red arrows) and stable intersections (red arrowheads) between nonregressing vessel segments at P21 in the deep plexus of the indicated genotypes. Scale bars represent 50 μm (except in A, 100 μm). (J-K) Quantitation of stable intersections (J) and regression profiles (K) in the deep plexus at P21; $n = 3$. Error bars represent SD of the mean. P values were determined by comparing the measurements obtained for both types of mutants to the control, which contained the measurements obtained for wild-types from both groups. SP indicates superficial plexus; IP, intermediate plexus; DP, deep plexus; ONL, outer nuclear layer; INL, inner nuclear layer; RGC, retinal ganglion cell layer; OPL, outer plexiform layer; PR, photoreceptor layer; a, artery; and v, vein.

to form the intermediate plexus around the second week after birth and then the deep vascular plexus in the third week (Figure 7B).⁴⁵ We observed that endothelial tip cells at the sprouting front of the retinal vasculature were in close contact with ramified tissue macrophages (microglia; solid arrows in Figure 7C). Moreover, macrophages bridged neighboring sprouts while they were anastomosing (wavy arrows in Figure 7C), as observed in the developing hindbrain (Figures 1-2). The interaction of tissue macrophages and endothelial cells is therefore similar in the hindbrain and retina, even though retinal macrophages appeared morphologically more differentiated.

A recently published study reported that *Csf1^{Op/Op}* mice form a superficial retinal plexus that is less complex than that of wild-types on postnatal day (P) 4, but that vascular density was normal at 3 weeks of age.⁹ Because macrophages control endothelial cell death during the natural regression of the hyaloid arteries,⁴⁶ we asked if normalization of the retinal vasculature in *Csf1^{Op/Op}* mutants was due to reduced remodeling. We found that regressing vessels in the superficial plexus of the wild-type retina could be identified by the presence of activated caspase 3 (Figure 7E), but also morphologically by their reduced diameter. Thus, vessel segments began to narrow first at the junction with other vessels (clear arrowheads in Figure 7E) and subsequently became thin,

acellular capillaries that retained collagen IV and IB4 (feathered arrows in Figure 7F). As expected, macrophages were often associated with regressing vessels (arrow in Figure 7E). At P9, regressing vessel segments were prominent near arteries, where capillary-free spaces arise (Figure 7D-F).⁴⁵ Similar regression profiles were found in the wild-type intermediate plexus at P14 (not shown) and in the deep plexus at P21 (Figure 7G).

Because the deep plexus forms the more extensive and homogeneous capillary bed of the 3 retinal vessel networks, we compared remodeling in macrophage-deficient and normal mice in this vascular bed (Figure 7G-J). We found that the deep plexus of *Csf1^{Op/Op}* mutants and their wild-type littermates contained a similar number of intersections between stable, lumenized microvessels of regular diameter (Figure 7J; compare Figure 7G with Figure 7H); however, the number of regressing, acellular capillaries was significantly lower in *Csf1^{Op/Op}* mutant eyes (Figure 7K; compare Figure 7G with H). We obtained similar results when we examined the deep plexus of PU.1-deficient mice, which had survived the perinatal period with a small number of macrophages (Figure 7I-K; 3/12 *Pu.1*-null neonates from 8 litters containing a total of 41 pups on the C57/BL6 background were alive at P21 with incisor defects similar to *Csf1^{Op/Op}* mice, but no other gross anatomical deficiencies). Together, these results suggest that a reduced number of

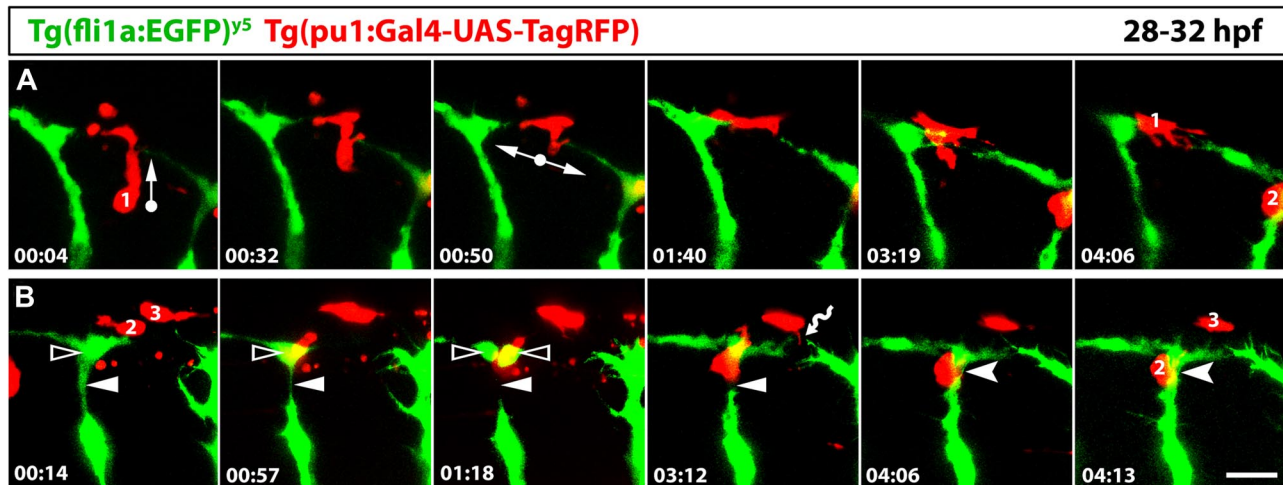


Figure 8. Tissue macrophages interact with endothelial cells at sites of vessel fusion in the developing zebrafish trunk. Series of laser confocal projections extracted from a time-lapse video (supplemental Video 1) showing the interaction of 3 tissue macrophages (red; 1-3) with blood vessels (green); the time elapsed after starting the video at 28 hpf is indicated in hours:minutes in the bottom left of each panel; 3 adjacent intersegmental blood vessels are imaged over a period of 4:16. (A) A macrophage (1) migrates into a region where the tip cell from the caudal sprout of one intersomitic vessel fuses with the tip cell of a rostral sprout of the next intersomitic vessel; arrows indicate the direction of macrophage migration. (B) A macrophage (2) migrates to a site where a dividing endothelial cell in the forming DLAV (clear arrowhead) transiently loses contact with the intersomitic vessel (arrowheads); it remains in this position while the connection is re-established (forked arrowheads); yet another macrophage (3) interacts with filopodial protrusions from opposing tip cells (wavy arrow). Scale bar represents 50 μm .

vessel intersections in macrophage-deficient mice at early stages of retinal development were balanced by a compensatory decrease in vessel pruning at later stages, and that the developing vasculature therefore becomes normalized by an adaptation of vascular remodeling.

Live imaging in zebrafish confirms a role for tissue macrophages in developmental angiogenesis

The morphologic and genetic data described above support a role for tissue macrophages in vascular anastomosis. To directly visualize the behavior of macrophages during vessel fusion and extend our findings to another model organism, we performed live imaging of vascular fusion sites in the developing zebrafish. To identify tissue macrophages, we modified a previously published DNA construct²⁴ to express RFP under the control of the macrophage *Pu.1* promoter and injected it into zebrafish embryos containing green fluorescent blood vessels.²⁵ We then imaged the process by which bilateral intersomitic blood vessels grow dorsally, branch laterally and fuse with branches from neighboring intersomitic vessels to form the dorsal longitudinal anastomotic vessel (DLAV) on each side of the trunk.⁴⁷ We observed that tissue macrophages migrated to sites of vessel fusion, where they interacted with endothelial cells (Figure 8, showing individual frames from supplemental Video 1). Figure 8A shows a macrophage that migrated toward a site of imminent anastomosis, where it changed direction to spread laterally and contact opposing tip cells (macrophage no. 1); the macrophage remained associated with both tip cells during the process of vessel fusion. Figure 8B shows an adjacent field of the same video, where another macrophage (no. 2) interacted with 2 vessel segments that were transiently severed during an endothelial cell mitosis. Thus, as the dividing cell in the DLAV (clear arrowhead) lost contact with the adjacent intersomitic vessel (arrowhead), this macrophage bridged the vascular gap until both vessel segments were reconnected (forked arrowhead). Figure 8B also shows another macrophage (no. 3), which extended processes to dynamically interact with tip

cell filopodia in the youngest part of this region (wavy arrow). These findings establish that macrophages interact with endothelial tip cells during vascular anastomosis in the zebrafish trunk. Moreover, they suggest that tissue macrophages are important for angiogenesis in several vascular beds and across different vertebrate species.

Discussion

Even though several subsets of macrophages have been implicated in pathologic angiogenesis, little attention has so far been paid to the significance of macrophage heterogeneity for physiologic tissue vascularization. While many types of adult macrophages involved in pathologic angiogenesis originate from bone marrow-resident hematopoietic stem cells via circulating monocytes, the first macrophages differentiate in the embryo without a monocytic intermediate and persist into adulthood as tissue macrophages.²⁷⁻³⁰ Yet the role of these early tissue macrophages in embryonic angiogenesis has not previously been explored. In this report, we show that they promote vascular networking.

For our studies, we concentrated on the embryonic hindbrain, because this organ is particularly amenable to the quantitative and qualitative analysis of angiogenesis, and because it is colonized by yolk sac-derived macrophages independently of blood vessels (supplemental Figure 1).^{31,36,48} These early macrophages give rise to the self-renewing parenchymal microglia of adults⁴⁹ and are distinct from adult perivascular macrophages, which differentiate from bone marrow-derived monocytic precursors.⁵⁰ We found embryonic tissue macrophages in close spatiotemporal association with sprouting vessels in the brain (supplemental Figure 1; Figures 1-2). Because tissue macrophages are highly motile cells that do not reside in any particular space for long,⁵¹ we were intrigued by the ease with which we captured their simultaneous interaction with one or more spatially well-separated tip cells (Figures 1-2,6). We found that macrophages also associated with endothelial tip

cells during retinal angiogenesis (Figure 7C) and during vessel fusion in the zebrafish trunk (Figure 8).

Because our observations further raised the possibility that macrophages interact with multiple tip cells to bring them into close apposition for fusion, we next investigated if macrophages were essential regulators of either tip cell formation or vessel anastomosis. We found that mice lacking PU.1 or CSF1 were appropriate models to study the role of macrophages in angiogenesis, because PU.1 loss prevented the differentiation of yolk sac–derived tissue macrophages throughout the embryo, and CSF1 loss prevented their recruitment from the head mesenchyme into the brain parenchyma (supplemental Figures 2-3). The idea that CSF1, but not VEGF164, is an essential recruitment factor for embryonic macrophages in the mouse brain (supplemental Figure 3; Figure 4) agrees with observations made of zebrafish *panther* mutants, which lack a functional CSF1 receptor. In these fish, tissue macrophages differentiate and migrate into the head mesenchyme, but macrophage recruitment into the brain is impaired.⁴⁸

Having established that PU.1- and CSF1-deficient mice provided suitable genetic models to uncover essential roles for tissue macrophages in angiogenesis, we first studied brain vascularization in these mice. We found that brain vascular complexity was decreased in both types of mutants (Figures 3,5; supplemental Figures 2-3). Importantly, the observed defects were qualitatively and quantitatively different from those of 2 different types of *Vegfa* mutants (Figures 3-4). Moreover, the exacerbation of vascular defects in mouse mutants defective in both VEGF signaling and macrophages (Figure 5) suggested that the 2 different mutations affect different steps in angiogenesis: whereas VEGF is particularly important for vessel sprouting, macrophages act on nascent sprouts to increase vascular anastomosis (Figure 5H). A similar decrease in vascular complexity was also seen in the retina of perinatal macrophage-deficient mice (data not shown).⁹

It is likely that the vascular defect we observed in macrophage-deficient mice underestimates the true significance of macrophages in normal angiogenesis, as is the case for embryonic footplate limb remodeling. There, macrophages normally clear the cellular debris that arises from the synchronous apoptosis of mesenchymal cells in the interdigital regions to facilitate digit separation; however, neighboring mesenchymal cells substitute for macrophages in *Pu.1*-null mutants to clear the apoptotic debris, although less effectively.⁵² In analogy, embryos with a genetic deficiency in tissue macrophages may activate compensatory mechanisms to promote vessel fusion. Moreover, emerging vascular networks appear sufficiently plastic to meet the physiologic need of the organism, as the overproduction of microvessels seems to be a normal process that is balanced by pruning of excess vessel circuits, either because they reside near arteries or because they are poorly perfused. Thus, we have shown that the elimination of excess vessel segments is reduced in macrophage-deficient mice (Figure 7), and we can therefore now explain why the retinal vasculature of CSF1 mutants, even though initially of low complexity, ultimately acquires a normal capillary density.⁹

Our observation that macrophage-mediated vessel fusion is most important in circumstances of suboptimal vessel growth (Figure 5) may explain why macrophage recruitment makes a significant contribution to pathologic angiogenesis. For example, macrophages trigger the angiogenic switch in cancer, because they help to establish a tumor vasculature, which then

allows tumors to overcome a “bottleneck” for growth that is due to insufficient oxygen and nutrient supply.^{5,6} Interestingly, the proangiogenic tissue macrophages we describe here do not normally express *Lysm* (supplemental Figure 4) and do not provide a significant source of VEGF (Figure 4), 2 features that distinguish them functionally from one class of VEGF-secreting, monocyte-derived inflammatory tumor-associated macrophages (TAMs) that promote tumor angiogenesis.⁵³ Instead, the tissue macrophages we characterize here (Figures 4,6) are similar to a second class of adult monocyte-derived proangiogenic tumor macrophages known as TEMs, which do not up-regulate either *Vegfa* or inflammatory genes, but do express TIE2 and NRP1.¹³ Interestingly, macrophages similar to adult TEMs were also identified in the embryo, but they were not enriched in the liver, where the first monocyte-derived macrophages originate; instead, they were abundant in the mesenchyme surrounding developing organs,¹³ like the proangiogenic macrophages we have characterized here.

To understand the cellular mechanisms that underlie macrophage function in vascular networking, we first investigated if macrophages stimulated vessel sprouting, but found that this was not the case (Figure 3). Because macrophages have the capacity to interact with more than one endothelial tip cell at a time (Figures 1G, 2A,C, 6C, 7C, and 8), we next considered that macrophages prime neighboring endothelial tip cells for fusion. Whereas virtually nothing is known about endothelial fusion in the vasculature, live imaging of dorsal closure in the *Drosophila* larva revealed that filopodia from opposing epithelial sheets project toward each other and form adhesive tethers, which align the cells in preparation for fusion.⁵⁴ In analogy, the filopodia that extend from tip cells at the front of blood vessel sprouts may initiate vessel fusion, if they make contact with each other. However, new vessel sprouts find themselves among a large number of nonendothelial cells in their host organ, hampering the process of finding a suitable fusion partner. Tissue macrophages, with their great mobility and flexibility and their affinity for tip-cell filopodia, therefore appear ideally suited to help endothelial cells on different vessel segments to establish contact. Consistent with this idea, we observed that tissue macrophages accumulated at sites of vessel fusion in the living zebrafish embryo, where they interacted with neighboring tip cells during the fusion process (Figure 8). Thus, by bridging tip cells from different vessel segments and embracing nascent fusion sites, macrophages can act as cellular chaperones for endothelial cell fusion to increase vascular complexity.

Acknowledgments

We thank Drs Scott R. McKercher, Napoleone Ferrara, David T. Shima, Juan-Pedro Martinez Barbera, and W. Zhong for providing mouse strains and the staff of the Biological Resources Unit at the UCL Institute of Ophthalmology for help with mouse husbandry. We are grateful to Kathryn Davidson for help with genotyping, Jenny McKenzie and Peter Munro for helpful technical advice, Tim Chico for sharing of unpublished data, and Matthew Golding for helpful comments on the manuscript.

This study was supported by a PhD studentship from the Fundação para a Ciência e Tecnologia (SFRH/BD/17812/2004) to J.M.V., research funding from the Medical Research Council to

C.R. (ref. G0601093) and to G.G. and S.W.W. (ref. G0900994), funding from The Wellcome Trust to S.W.W. (ref. 088175/Z09/Z), and a PhD studentship from the British Heart Foundation to A.F. (ref. 44626).

Authorship

Contribution: A.F., J.M.V., and G.G. designed and performed research and analyzed data; L.D. and Q.S. performed research; S.P. and F.P. provided vital reagents; S.W.W. designed research and

analyzed data; and C.R. designed and performed research, analyzed data, and wrote the manuscript.

Conflict-of-interest disclosure: The authors declare no competing financial interests.

The current affiliation for J.M.V. is UCL Institute of Child Health, University College London, London, United Kingdom. The current affiliation for Q.S. is Department of Human Immunology, Centre for Cancer Biology, Adelaide, Australia.

Correspondence: Christiana Ruhrberg, UCL Institute of Ophthalmology, University College London, 11-43 Bath St, London EC1V 9EL, United Kingdom; e-mail: c.ruhrberg@ucl.ac.uk.

References

- Ruhrberg C, Gerhardt H, Golding M, et al. Spatially restricted patterning cues provided by heparin-binding VEGF-A control blood vessel branching morphogenesis. *Genes Dev*. 2002; 16(20):2684-2698.
- Gerhardt H, Golding M, Fruttiger M, et al. VEGF guides angiogenic sprouting utilizing endothelial tip cell filopodia. *J Cell Biol*. 2003;161(6):1163-1177.
- Affolter M, Zeller R, Caussinus E. Tissue remodeling through branching morphogenesis. *Nat Rev Mol Cell Biol*. 2009;10(12):831-842.
- Grunewald M, Avraham I, Dor Y, et al. VEGF-induced adult neovascularization: recruitment, retention, and role of accessory cells. *Cell*. 2006; 124(1):175-189.
- Pollard JW. Tumour-educated macrophages promote tumour progression and metastasis. *Nat Rev Cancer*. 2004;4(1):71-78.
- Lin EY, Pollard JW. Tumor-associated macrophages press the angiogenic switch in breast cancer. *Cancer Res*. 2007;67(11):5064-5066.
- Luttun A, Tjwa M, Moons L, et al. Revascularization of ischemic tissues by PIGF treatment, and inhibition of tumor angiogenesis, arthritis and atherosclerosis by anti-Flt1. *Nat Med*. 2002;8(8): 831-840.
- Pipp F, Heil M, Issbrucker K, et al. VEGFR-1-selective VEGF homologue PIGF is arteriogenic: evidence for a monocyte-mediated mechanism. *Circ Res*. 2003;92(4):378-385.
- Kubota Y, Takubo K, Shimizu T, et al. M-CSF inhibition selectively targets pathological angiogenesis and lymphangiogenesis. *J Exp Med*. 2009; 206(5):1089-1102.
- Checchin D, Sennlaub F, Levavasseur E, Leduc M, Chemtob S. Potential role of microglia in retinal blood vessel formation. *Invest Ophthalmol Vis Sci*. 2006;47(8):3595-3602.
- Espinosa-Heidmann DG, Suner IJ, Hernandez EP, Monroy D, Csaky KG, Cousins SW. Macrophage depletion diminishes lesion size and severity in experimental choroidal neovascularization. *Invest Ophthalmol Vis Sci*. 2003;44(8):3586-3592.
- Sakurai E, Anand A, Ambati BK, van Rooijen N, Ambati J. Macrophage depletion inhibits experimental choroidal neovascularization. *Invest Ophthalmol Vis Sci*. 2003;44(8):3578-3585.
- Pucci F, Venneri MA, Bizzi D, et al. A distinguishing gene signature shared by tumor-infiltrating Tie2-expressing monocytes (TEMs), blood "resident" monocytes and embryonic macrophages suggests common functions and developmental relationships. *Blood*. 2009;114(4):901-914.
- Sato TN, Tozawa Y, Deutsch U, et al. Distinct roles of the receptor tyrosine kinases Tie-1 and Tie-2 in blood vessel formation. *Nature*. 1995; 376(6535):70-74.
- Fantin A, Maden CH, Ruhrberg C. Neuropilin ligands in vascular and neuronal patterning. *Biochem Soc Trans*. 2009;37(Pt 6):1228-1232.
- McKercher SR, Torbett BE, Anderson KL, et al. Targeted disruption of the PU. 1 gene results in multiple hematopoietic abnormalities. *EMBO J*. 1996;15(20):5647-5658.
- Wiktor-Jedrzejczak W, Bartocci A, Ferrante AW Jr, et al. Total absence of colony-stimulating factor 1 in the macrophage-deficient osteopetrotic (op/op) mouse. *Proc Natl Acad Sci U S A*. 1990; 87(12):4828-4832.
- Yoshida H, Hayashi S, Kunisada T, et al. The murine mutation osteopetrosis is in the coding region of the macrophage colony stimulating factor gene. *Nature*. 1990;345(6274):442-444.
- Gerber HP, Hillan KJ, Ryan AM, et al. VEGF is required for growth and survival in neonatal mice. *Development*. 1999;126(6):1149-1159.
- Clausen BE, Burkhardt C, Reith W, Renkawitz R, Forster I. Conditional gene targeting in macrophages and granulocytes using LysMcre mice. *Transgenic Res*. 1999;8(4):265-277.
- Petersen PH, Zou K, Hwang JK, Jan YN, Zhong W. Progenitor cell maintenance requires numb and numblike during mouse neurogenesis. *Nature*. 2002;419(6910):929-934.
- Srinivas S, Watanabe T, Lin CS, et al. Cre reporter strains produced by targeted insertion of EYFP and ECFP into the ROSA26 locus. *BMC Dev Biol*. 2001;1:4.
- Ivanova A, Signore M, Caro N, Greene ND, Copp AJ, Martinez-Barbera JP. In vivo genetic ablation by Cre-mediated expression of diphtheria toxin fragment A. *Genesis*. 2005;43(3):129-135.
- Peri F, Nusslein-Volhard C. Live imaging of neuronal degradation by microglia reveals a role for v0-ATPase a1 in phagosomal fusion in vivo. *Cell*. 2008;133(5):916-927.
- Lawson ND, Weinstein BM. In vivo imaging of embryonic vascular development using transgenic zebrafish. *Dev Biol*. 2002;248(2):307-318.
- Peirson SN, Butler JN, Foster RG. Experimental validation of novel and conventional approaches to quantitative real-time PCR data analysis. *Nucleic Acids Res*. 2003;31(14):e73.
- Herbomel P, Thisse B, Thisse C. Ontogeny and behaviour of early macrophages in the zebrafish embryo. *Development*. 1999;126(17):3735-3745.
- Lichanska AM, Hume DA. Origins and functions of phagocytes in the embryo. *Exp Hematol*. 2000; 28(6):601-611.
- Sorokin SP, Hoyt RF Jr, Blunt DG, McNelly NA. Macrophage development: II. Early ontogeny of macrophage populations in brain, liver, and lungs of rat embryos as revealed by a lectin marker. *Anat Rec*. 1992;232(4):527-550.
- Cuadros MA, Martin C, Coltey P, Almendros A, Navascues J. First appearance, distribution, and origin of macrophages in the early development of the avian central nervous system. *J Comp Neurol*. 1993;330(1):113-129.
- Kurz H, Christ B. Embryonic CNS macrophages and microglia do not stem from circulating, but from extravascular precursors. *Glia*. 1998;22(1): 98-102.
- Austyn JM, Gordon S. F4/80, a monoclonal antibody directed specifically against the mouse macrophage. *Eur J Immunol*. 1981;11(10):805-815.
- Imai Y, Ibata I, Ito D, Ohsawa K, Kohsaka S. A novel gene *iba1* in the major histocompatibility complex class III region encoding an EF hand protein expressed in a monocytic lineage. *Biochem Biophys Res Commun*. 1996;224(3):855-862.
- Simon MC. PU. 1 and hematopoiesis: lessons learned from gene targeting experiments. *Semin Immunol*. 1998;10(2):111-118.
- Scott EW, Simon MC, Anastasi J, Singh H. Requirement of transcription factor PU. 1 in the development of multiple hematopoietic lineages. *Science*. 1994;265(5178):1573-1577.
- Lichanska AM, Browne CM, Henkel GW, et al. Differentiation of the mononuclear phagocyte system during mouse embryogenesis: the role of transcription factor PU. 1. *Blood*. 1999;94(1):127-138.
- Olson MC, Scott EW, Hack AA, et al. PU. 1 is not essential for early myeloid gene expression but is required for terminal myeloid differentiation. *Immunity*. 1995;3(6):703-714.
- Chang MD, Stanley ER, Khallil H, Chisholm O, Pollard JW. Osteopetrotic (op/op) mice deficient in macrophages have the ability to mount a normal T-cell-dependent immune response. *Cell Immunol*. 1995;162(1):146-152.
- Webb SE, Pollard JW, Jones GE. Direct observation and quantification of macrophage chemotaxis to the growth factor CSF-1. *J Cell Sci*. 1996;109(Pt 4):793-803.
- Barleon B, Sozzani S, Zhou D, Weich HA, Mantovani A, Marme D. Migration of human monocytes in response to vascular endothelial growth factor (VEGF) is mediated via the VEGF receptor flt-1. *Blood*. 1996;87(8):3336-3343.
- Haigh JJ, Morelli PI, Gerhardt H, et al. Cortical and retinal defects caused by dosage-dependent reductions in VEGF-A paracrine signaling. *Dev Biol*. 2003;262(2):225-241.
- Raab S, Beck H, Gaumann A, et al. Impaired brain angiogenesis and neuronal apoptosis induced by conditional homozygous inactivation of vascular endothelial growth factor. *Thromb Haemost*. 2004;91(3):595-605.
- Miquerol L, Gertsenstein M, Harpal K, Rossant J, Nagy A. Multiple developmental roles of VEGF suggested by a LacZ-tagged allele. *Dev Biol*. 1999;212(2):307-322.
- Hiratsuka S, Maru Y, Okada A, Seiki M, Noda T, Shibuya M. Involvement of Flt-1 tyrosine kinase (vascular endothelial growth factor receptor-1) in pathological angiogenesis. *Cancer Res*. 2001; 61(3):1207-1213.
- Connolly SE, Hores TA, Smith LE, D'Amore PA. Characterization of vascular development in the

- mouse retina. *Microvasc Res*. 1988;36(3):275-290.
46. Rao S, Lobov IB, Vallance JE, et al. Obligatory participation of macrophages in an angiopoietin 2-mediated cell death switch. *Development*. 2007;134(24):4449-4458.
 47. Isogai S, Lawson ND, Torrealday S, Horiguchi M, Weinstein BM. Angiogenic network formation in the developing vertebrate trunk. *Development*. 2003;130(21):5281-5290.
 48. Herbomel P, Thisse B, Thisse C. Zebrafish early macrophages colonize cephalic mesenchyme and developing brain, retina, and epidermis through a M-CSF receptor-dependent invasive process. *Dev Biol*. 2001;238(2):274-288.
 49. Chan WY, Kohsaka S, Rezaie P. The origin and cell lineage of microglia: new concepts. *Brain Res Rev*. 2007;53(2):344-354.
 50. Bechmann I, Priller J, Kovac A, et al. Immune surveillance of mouse brain perivascular spaces by blood-borne macrophages. *Eur J Neurosci*. 2001;14(10):1651-1658.
 51. Herbomel P, Levraud JP. Imaging early macrophage differentiation, migration, and behaviors in live zebrafish embryos. *Methods Mol Med*. 2005;105:199-214.
 52. Wood W, Turmaine M, Weber R, et al. Mesenchymal cells engulf and clear apoptotic footplate cells in macrophageless PU. 1 null mouse embryos. *Development*. 2000;127(24):5245-5252.
 53. Stockmann C, Doedens A, Weidemann A, et al. Deletion of vascular endothelial growth factor in myeloid cells accelerates tumorigenesis. *Nature*. 2008;456(7223):814-818.
 54. Millard TH, Martin P. Dynamic analysis of filopodial interactions during the zipper phase of *Drosophila* dorsal closure. *Development*. 2008;135(4):621-626.